PSFC/JA-00-28

Plasma Curvature Effects on Microwave Reflectometry Fluctuation Measurements

Y. Lin, R. Nazikian[1], J.H. Irby, E.S. Marmar

September 2000

Plasma Science and Fusion Center
Massachusetts Institute of Technology
Cambridge, MA 02139 USA

[1]Princeton Plasma Physics Laboratory, Princeton, NJ 08543

This work was supported by the U.S. Department of Energy, Cooperative Grant No. DE-FC02-99ER54512. Reproduction, translation, publication, use and disposal, in whole or in part, by or for the United States government is permitted.

Submitted for publication to *Plasma Phys. and Control. Fusion.*

Plasma curvature effects on microwave reflectometry fluctuation measurements

Y. Lin*, R. Nazikian†, J.H. Irby, E.S. Marmar

MIT, Plasma Science and Fusion Center, Cambridge, MA 02139, USA

†*Princeton Plasma Physics Laboratory, Princeton, NJ 08543, USA*

Abstract

Plasma poloidal curvature can significantly extend microwave reflectometry responses to high $k_\perp$ poloidal fluctuations. Reflectometry responses can be several orders of magnitude larger at high $k_\perp$ than that predicted by analysis based on two dimensional (2-D) slab geometry. As a result, the responses may approach the 1-D geometrical optics limit. This super resolution leads to a major modification of the spectral resolution of reflectometry. The phenomenon is analyzed using a phase screen model for the general cases and the results are supported by detailed numerical 2-D realistic geometry full wave simulations for the specific case of the Alcator C-Mod tokamak.

*Email: ylin@psfc.mit.edu

Reflectometry is now a widely used tool for interpreting the behavior of plasma profiles and as an indicator of the properties of plasma density fluctuations. A number of simplified scattering models exist which reproduce important features of reflectometer measurements, however there is still an incomplete description of the scattering process incorporating real plasma geometry and antenna structures. Such analysis using full wave simulation is needed in order to establish reflectometry as a quantitative diagnostic for fluctuation measurements in fusion plasmas. In this letter we show that the inclusion of the effect of plasma curvature into the full wave analysis of the reflectometer response to poloidal fluctuations can lead to a major modification of the spectral resolution compared to analysis based on slab geometry. In previous studies, various two-dimensional (2-D) models have been developed to interpret reflectometry responses to poloidal density fluctuations [1]-[7]. 2-D analytical studies have also been performed on linear density profiles [8]. These 2-D models or analytical studies are either based on slab plasma profiles [2]-[8], or do not isolate and clarify the effect of plasma curvature where it is included [1]. It is well known that the reflectometry sensitivity to poloidal fluctuation wavenumber, $k_\perp$, is limited by receiver location and incident beam width (or spot size). For a finite beam width it was shown that the geometric optics result in 1-D may apply for $k_\perp w \ll \pi/\sqrt{2}$, where w is $1/e$ radius of the incident beam intensity (reference [4]). For larger wavenumbers, it was suggested that a tilted receiver arrangement is necessary for measuring fluctuations with $k_\perp w \gg \pi/\sqrt{2}$. The issue of resolution has also been addressed using the distorted mirror model [5] [6], assuming that the receiver and transmitter have similar aperture sizes. This analysis showed that the

upper limit for the undistorted observation of the poloidal spectrum is $k_\perp w \leq \pi/5$. It was suggested in reference [6] that a tightly focused beam is better for fluctuations measurement in order to enhance the gain and improve the wavenumber response. A $1/e^2$ sensitivity criterion of the reflectometry, $k_\perp w < 2$, can be deduced from the result of a rigorous analysis based on slab geometry and linear density profiles [8].

However, in experiments on Alcator C-Mod we have found the surprising result that the reflectometer system seems to be sensitive to poloidal wavelengths much shorter than is suggested by the above studies. For instance, the reflectometer (O-mode, 88 GHz, the wavenumber in vacuum $k_0 \simeq 18.5$ cm^{-1}) in the Alcator C-Mod tokamak is clearly sensitive to high $k_\perp$ quasi-coherent fluctuations ($60 - 250$ kHz in lab frame) in the Enhanced D_α (EDA) H-mode plasma pedestal region [9]-[13]. The $k_\perp$ of the quasi-coherent fluctuations are in the range $k_\perp \simeq 4 - 8$ cm^{-1} as determined by the phase contrast imaging (PCI) system. PCI measures line-integrated density fluctuations along 12 vertical chords passing through the plasma at the same toroidal location but different radial positions such that it is sensitive to k_θ for mode localized to the plasma edge [13]. The reflectometer views along the plasma mid-plane so that for edge localized measurements we have $k_\theta = k_\perp$. On the other hand the reflectometer antenna spot size at the cutoff is estimated to be $w \sim 1 - 2$ cm, with receiver distance $d \simeq 20$ cm, horn antenna angles $\pm 5^0$ relative to the mid-plane. The observed system response appears to be much broader in $k_\perp$ than predicted from 2-D slab geometry analysis for these plasmas [13].

In this letter, we show that super-resolution of high $k_\perp$ fluctuations can indeed

be achieved due to a magnification caused by plasma poloidal curvature and the curved wave-front of the incident waves. The phenomenon of super resolution is analyzed using a phase screen model for general cases and the results are supported by detailed numerical 2-D full wave simulations for the specific case of the Alcator C-Mod tokamak. Implications for experiments on other devices are discussed, as well as criteria for the validity of 1-D geometric optics for determining the sensitivity of reflectometry to poloidal fluctuations.

To give a general insight into the curvature effect, we use a phase screen model including plasma curvature and wave-front curvature (figure 1). All plasma effects are reduced to the phase modulation induced by the phase screen. The phase of the electric field at the screen is calculated by 1-D geometrical optics: $\phi_0 = 2k_0 \int_0^{z_c} \epsilon^{1/2}\, dz$, where ϵ is plasma permittivity, z_c is the critical layer, $z = 0$ at the plasma edge, and k_0 is the incident microwave vacuum wavenumber. The phase screen is located at $z_s = \int_0^{z_c} \epsilon^{-1/2}\, dz$, i.e., at the effective optical distance from the plasma edge. A poloidal plasma density fluctuation is modeled as a phase modulation with wavenumber $k_\perp$. The modulation magnitude, $\sigma_\phi = \langle(\phi - \phi_0)^2\rangle^{1/2}$, can also be calculated from 1-D geometric optics given the details of the density profile. Assuming a radius of curvature ρ_c of the cutoff layer and ρ_w of the incident wave-front at the cutoff layer, the complex electric field at the phase screen is approximately:

$$E_s(\xi) = \frac{1}{\sqrt{2\pi}w} \exp\left(-\frac{\xi^2}{2w^2}\right) \times \exp\left(\frac{ik_0\xi^2}{\rho}\right) \times \exp\left[i\sqrt{2}\sigma_\phi \cos(k_\perp \xi + \theta)\right] \qquad (1)$$

where ξ is the coordinate on the phase screen, θ is the phase offset of the modulation at $\xi = 0$, $\rho = 2\rho_c\rho_w/(\rho_c + 2\rho_w)$ is the effective radius of curvature, and w is the $1/e$

radius of the Gaussian incident waves intensity ($\propto |E_s|^2$) distributed on the phase screen. The second term comes from the curvature effect assuming $w \ll \rho/2$. The third term denotes phase modulation by density fluctuations.

The electric field in all space, in principle, can be calculated using the Fresnel-Huygens formula:

$$\begin{aligned} E(y,z) &= \frac{1}{2\pi}\int_{-\infty}^{\infty} g(u)\exp\left[i(z-z_s)\sqrt{k_0^2-u^2}\right]\exp(iuy)\ du \\ g(u) &= \int_{-\infty}^{\infty} E_s(\xi)\exp(-iu\xi)\ d\xi \end{aligned} \tag{2}$$

Only two dimensions of the formula is incorporated. In the regime where $\sigma_\phi \ll 1$, $k_\perp \ll k_0$, we estimate the rms level of the electric field over $-\pi < \theta < \pi$ on the axis $y = 0$. By integrating equation 2, we find:

$$\begin{aligned} E_{rms}(0,z) &= \frac{\langle |E-\langle E\rangle|^2\rangle^{1/2}}{|\langle E\rangle|} \simeq \sigma_\phi \exp\left[-\frac{k_\perp^2 w^2}{C_1}\left(1-\frac{1}{2}C_2\right)\right] \\ C_1 &= 1+\frac{4k_0^2 w^4}{\rho^2} \\ C_2 &= \frac{1-4d/\rho}{(1-2d/\rho)^2+d^2/k_0^2 w^4} \end{aligned} \tag{3}$$

where $d = z - z_s$ is the distance to the phase screen. The curvature effect is strongly embedded in parameter C_1 while C_2 is usually close to 1. In the case of $k_\perp \to 0$ or $w \to 0$, E_{rms} approaches σ_ϕ, which is the 1-D geometrical optics limit. In the regime of weak curvature where $\rho \gg 2k_0 w^2$, the curvature effect is negligible. Using $C_2 \simeq 1$, we get:

$$E_{rms}(0,z) \simeq \sigma_\phi \exp\left(-k_\perp^2 w^2/2\right), \quad \rho/2 \gg k_0 w^2 \tag{4}$$

The dependence on $\exp\left(-k_\perp^2 w^2/2\right)$ is identical to that deduced from the result in

reference [8]. In contrast, in the regime of strong curvature where $w \ll \rho/2 \ll k_0 w^2$,

$$E_{rms}(0,z) \simeq \sigma_\phi \exp\left[-\left(\frac{\rho}{2k_0w^2}\right)^2 \frac{k_\perp^2 w^2}{2}\right], \quad w \ll \rho/2 \ll k_0 w^2 \tag{5}$$

Equation 5 shows that, with strong curvature, the electric field fluctuations due to a density fluctuation with wavenumber $k_\perp$ is as strong as for density fluctuation of much smaller wavenumber,

$$k'_\perp \simeq \left(\frac{\rho}{2k_0w^2}\right) k_\perp, \quad w \ll \rho/2 \ll k_0 w^2 \tag{6}$$

found in equation 4, which is the analytical result using slab plasma geometry and plane wave-front with finite beam size. As a result, the reflectometry response to poloidal fluctuations can be significantly broader in $k_\perp$ than the result without consideration of plasma curvature.

Figure 2 shows E_{rms}/σ_ϕ calculated using equation 3 for different curvature radii. Figure 2-(a) is the case of $\rho_w = 10$ cm while $\rho_w = 25$ cm is shown in figure 2-(b). Results of plasma curvature $\rho_c = \infty$, 25 and 15 cm are plotted. Other parameters used are realistic parameters for the Alcator C-Mod 88 GHz reflectometer channel, $k_0 \simeq 18.5$ cm^{-1}, $w \simeq 1.6$ cm, $d \simeq 20$ cm. All curves converge to the 1-D geometric optics limit, $E_{rms}/\sigma_\phi = 1$, for $k_\perp \to 0$. For large $k_\perp$, there can be orders of magnitude difference in E_{rms} for different ρ_c. E_{rms}/σ_ϕ in figure 2-(a) is also larger than those in figure 2-(b) with the same ρ_c because of a smaller ρ_w.

A more realistic plasma curvature effect for O-mode reflectometry has been estimated using a 2-D full wave simulation based on the experimental density profile and reflectometer geometry in the Alcator C-Mod tokamak. The 2-D full wave code we use is an upgrade of the previous Maxwell code [1], which solves Maxwell's

equations for O-mode wave propagation under the assumption of a cold plasma. The new code uses the Huygens sources technique (reference [14]) to generate a Gaussian beam to simulate the launched microwave and also separates the reflected waves from the total field. Using a perfectly matched layer (reference [15]) as the boundary for the full wave simulation, the code has sufficient accuracy to simulate reflectometer fluctuation measurements with realistic density profiles and geometry [13]. The plasma density profile is modelled with an EDA H-mode profile with pedestal width of 0.6 cm at $z < 0$:

$$n_{e0}(z)/n_c = 0.8\left[1 - 0.025z - \tanh\left(\frac{z+3.5}{0.6}\right)\right] \tag{7}$$

where lengths are in cm, and $n_c = 0.96 \times 10^{14}$ cm^{-3} is the cutoff density for 88 GHz microwave (O-mode). The fluctuations are assumed to be localized in z but poloidally modulated:

$$\tilde{n}_e(z)/n_{e0} = 0.04 \times \exp\left[-\left(\frac{z+3.3}{0.35}\right)^2\right]\cos(k_\perp y + \theta) \tag{8}$$

Such fluctuations give a 1-D phase modulation level $\sigma_\phi \simeq 0.5$ rad. The total density is $n_e = n_{e0} + \tilde{n}_e$.

The electric field of the incident Gaussian beam in the vacuum region propagating in $-\vec{e}_z$ direction is described as (a time factor $e^{-i\omega t}$ is ignored):

$$E_b(y,z) \simeq \sqrt{\frac{2P}{\pi w_b^2}}\exp\left[-i\arctan\left(\frac{z-z_0}{k_0 w_0^2}\right) - y^2\left(\frac{1}{2w_b^2} + \frac{ik_0}{2\rho_b}\right)\right]\exp\left[-ik_0(z-z_0)\right] \tag{9}$$

where z_0 is the position of the beam waist and w_0 is the beam waist radius; the beam's $1/e$ intensity radius $w_b = w_0\left[1 + (z-z_0)^2/k_0^2 w_0^4\right]^{1/2}$; the radius of wavefront curvature $\rho_b = |z-z_0|\left[1 + k_0^2 w_0^4/(z-z_0)^2\right]$; P is the total incident power.

We assume a Gaussian beam waist radius $w_0 \simeq 0.75$ cm at the launching horn aperture position ($z_0 \simeq 15$ cm), which has an optical distance $d \simeq 20$ cm to the cutoff layer based on the model density profile. We estimate $\rho_b \simeq 25$ cm and $w_b \simeq 1.6$ cm at the phase screen based on the propagation in vacuum.

Figure 3 and figure 4 show the 2-D electric field distribution of $\rho_c = \infty, 25,$ and 15 cm for a single-antenna system (figure 3) and a two-antenna (transmitter XMTR and receiver RCVR) system with angles of $\pm 5^0$ relative to $y = 0$ (figure 4). In the simulation, we construct a Huygens surface at $z = 2\pi/k_0 \simeq 0.34$ cm, and generate Gaussian beams propagating towards the plasma at $z < 0$. The Huygens surface separates the reflected waves from the total field. As a result, the field in the region of $z > 0.34$ cm consists of only the reflected waves while the total electric field of the incident Gaussian beam and the reflected waves are shown in the region of $z < 0.34$ cm in both figure 3 and 4. The contour level is $E = \frac{1}{2}E_0$, where E_0 is the maximal electric field amplitude at the Gaussian beam waist. The plasma density profile at $y = 0$ is also shown. The fluctuation wavenumber is $k_\perp = 6$ cm^{-1} and the phase modulation level $\sigma_\phi \simeq 0.5$ rad. With smaller ρ_c, the reflected waves are more poloidally expanded, which results in less absolute power received by RCVR.

The plasma density fluctuations perturb the electric field distribution and reflectometry derives the density fluctuations from the electric field perturbation. The electric field perturbation caused by the plasma density fluctuation is larger for smaller ρ_c. Figure 5 shows an enlarged view of the region near the antenna of figure 3. The contours of $\Re(\tilde{E})/|E|$ are plotted, where $\tilde{E}$ is the difference of the

electric fields with density fluctuations ($\sigma_\phi = 0.5$ rad) and without density fluctuations ($\sigma_\phi = 0$), and $|E|$ is the amplitude of the complex electric field. $\Re(\tilde{E})/|E|$ is poloidally modulated due to the poloidal density fluctuation. The perturbation level on the electric field is $\sigma_E = \langle|\tilde{E}|^2/|E|^2\rangle^{1/2}$, where average $\langle\ \rangle$ is defined in the region shown in the figure. The perturbation level increases for smaller ρ_c. $\sigma_E \simeq 0.13, 0.23$ and 0.28 is obtained for $\rho_c = \infty, 25$ and 15 cm respectively. This response is many orders of magnitude larger than expected from 2-D slab geometry analysis (equation 4), but much closer to the 1-D geometrical optics limit, $\sigma_E \simeq \sigma_\phi \simeq 0.5$. The larger σ_E shown in the case of curved plasma than that in the cases of $\rho_c = \infty$ means higher sensitivity to density fluctuations.

Including the finite size of the receiving horn antenna, the rms level of reflectometer response over a fluctuation period, E_{rms} is slightly less than σ_E. Figure 6 shows E_{rms}/σ_ϕ versus the poloidal wavenumber $k_\perp$. The results of the single-antenna system and two-antenna systems are similar. For a typical quasi-coherent fluctuations in the EDA H-mode, $k_\perp \simeq 6$ cm^{-1}, the simulation result shows that the reflectometer response with $\rho_c = 15$ cm (which is close to the EFIT reconstructed magnetic flux curvature radius) is over 10 times higher than that of a slab profile plasma with $\rho_c = \infty$. The simulation results are close to those in figure 2-(a), which are calculated from equation 3 using $\rho_w = 10$ cm. In contrast, the results in figure 2-(b), which is obtained using $\rho_w = \rho_b = 25$ cm, where ρ_b is the estimated Gaussian beam curvature radius at the phase screen based on propagation in vacuum, are much smaller than the simulation results. It indicates that the plasma effect on the wave-front curvature is not negligible when using the

phase screen model (equation 3) to estimate the reflectometry sensitivity. It also indicates that plasma curvature plays an important role in determining the wave number resolution of the measurement.

In conclusion, plasma curvature is found to significantly extend the microwave reflectometry response to high $k_\perp$ fluctuations when the effective radius of curvature $\rho \ll 2k_0w^2$. The reflectometry responses to high $k_\perp$ poloidal fluctuations may be several orders of magnitude larger than the slab geometry result. Thus, the 1-D model may work better than 2-D slab geometry models for high $k_\perp$ fluctuations due to the curvature effect. At low $k_\perp$, however, the 1-D model and 2-D slab geometry models agree well, and plasma curvature does not affect the response.

Acknowledgements

The work is supported by US-DOE D.o.E. Coop. Agreement DE-FC02-99ER54512 and DE-AC02-76-CHO-3073.

References

[1] J.H. Irby, S. Horne, I.H. Hutchinson, P.C. Stek, Plasma Phys. Control. Fusion **35**, 601-618 (1993).

[2] R. Nazikian and E. Mazzucato, Rev. Sci. Instrum. **66** (1), 392-398 (1995).

[3] E. Mazzucato, Rev. Sci. Instrum. **69** (4), 1691-1698 (1998).

[4] E. Holzhauer, M. Hirsch, T. Grossmann, B. Brañas and F. Serra, Plasma Phys. Control. Fusion **40**, 1869-1886 (1998).

[5] G.D. Conway, Plasma Phys. Control. Fusion **41**, 65-92 (1999).

[6] G.D. Conway, Plasma Phys. Control. Fusion **39**, 1261-1265 (1997).

[7] V. Zhuravlev. J. Sanchez and E. de la Luna, Plasma Phys. Control. Fusion **38**, 2231-2242 (1996).

[8] E.Z. Gusakov, M.A. Tyntarev, Fusion Engineering and Design **34-35**, 501-505 (1997).

[9] P.C. Stek, PhD dissertation, *Reflectometry Measurements on Alcator C-Mod*, Massachusetts Institute of Technology, March, 1997.

[10] Y. Lin, J. Irby, P. Stek, I. Hutchinson, J. Snipes, R. Nazikian, M. McCarthy, Rev. Sci. Instrum. **70** (1), 1078-1081 (1999).

[11] M. Greenwald, et al, Phys. Plasmas **6** (5), 1943-1949 (1999).

[12] M. Greenwald, et al, Plasma Phys. Control. Fusion **42**, A263-A269 (2000).

[13] Y. Lin, J. Irby, R. Nazikian, E.S. Marmar, A. Mazurenko, Rev. Sci. Instrum., December (2000). To be published.

[14] R. Holland and J.W. Williams, IEEE Transactions on Nuclear Science, Vol. NS-30, No. 6, 4583-4588, December, 1983.

[15] J. Berenger, J. of Computational Physics **114**, 185-200 (1994).

Captions:

Fig 1. The phase screen model with plasma curvature and curved wave-front.

Fig 2. E_{rms}/σ_ϕ evaluated from equation 3 for different radii of plasma curvature: $\rho_c = \infty$, 25 and 15 cm. $k_0 \simeq 18.5$ cm^{-1}, $w \simeq 1.6$ cm, $d \simeq 20$ cm. Figure (a) shows the result of $\rho_w = 10$ cm and figure (b) shows the result of $\rho_w = 25$ cm.

Fig 3. The distribution of the electric field for a single-antenna system. (a) slab geometry $\rho_c = \infty$, (b) curved plasma with $\rho_c = 25$ cm; (c) curved plasma with $\rho_c = 15$ cm. The cutoff layer and the antenna (XMTR/RCVR) are also drawn. The density profile at $y = 0$ is drawn in (d). The fluctuation $k_\perp = 6$ cm and $\sigma_\phi = 0.5$ rad.

Fig 4. The distribution of the electric field for a two-antenna system. (a) slab geometry $\rho_c = \infty$; (b) curved plasma with $\rho_c = 25$ cm; (c) curved plasma with $\rho_c = 15$ cm. The cutoff layer and the antennas (transmitter XMTR and receiver RCVR) are also drawn. Antenna angles are $\pm 5^0$ relative to $y = 0$ axis. The density profile at $y = 0$ is drawn in (d). The fluctuation $k_\perp = 6$ cm and $\sigma_\phi = 0.5$ rad.

Fig 5. $\Re(\tilde{E})/|E|$ in an enlarged region near the antenna for the single-antenna system in figure 3. (a) slab geometry $\rho_c = \infty$, (b) curved plasma with $\rho_c = 25$ cm. (c) curved plasma with $\rho_c = 15$ cm.

Fig 6. E_{rms}/σ_ϕ for different radii of curvature of plasma from the 2-D full wave simulation. $\rho_c = \infty, 25, 15$ cm. Figure (a) is for the single-antenna system (figure 3) and figure (b) is for the two-antenna system (figure 4).

Figures:

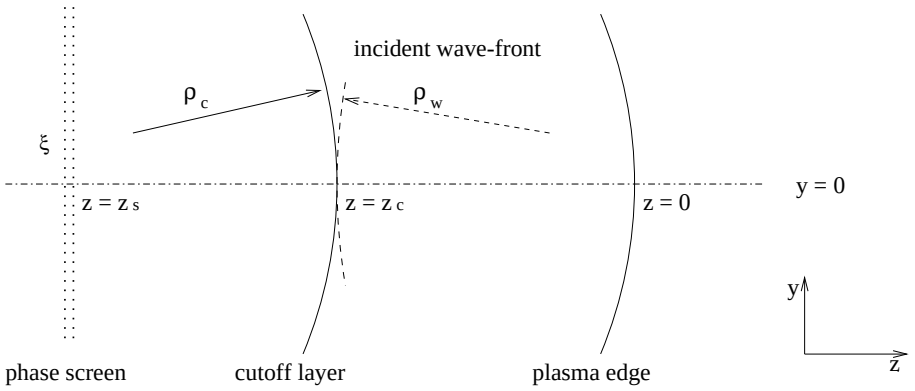

Figure 1: (Y. Lin)

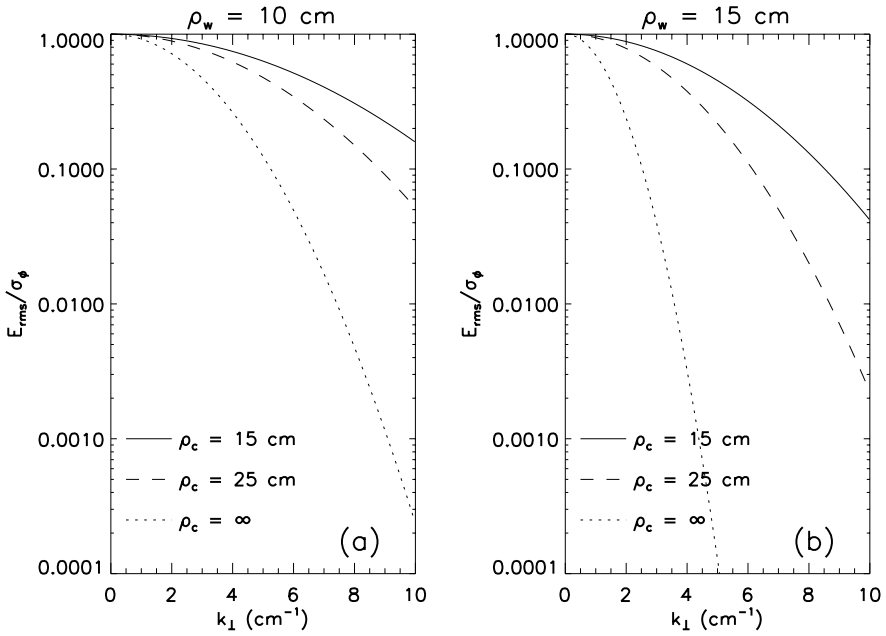

Figure 2: (Y. Lin)

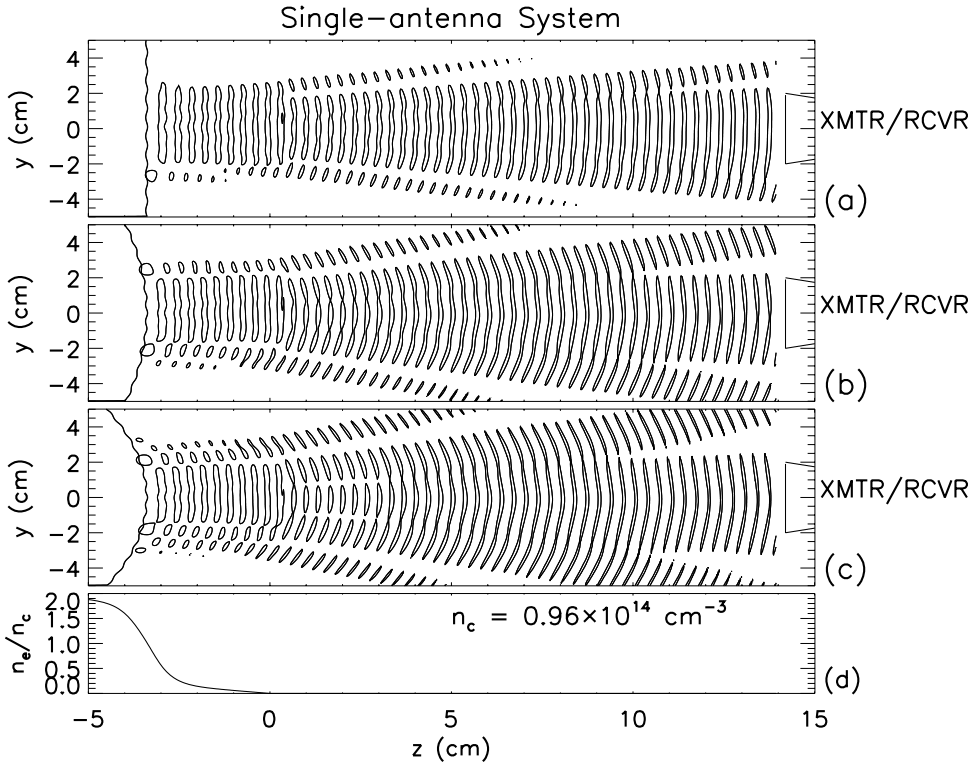

Figure 3: (Y. Lin)

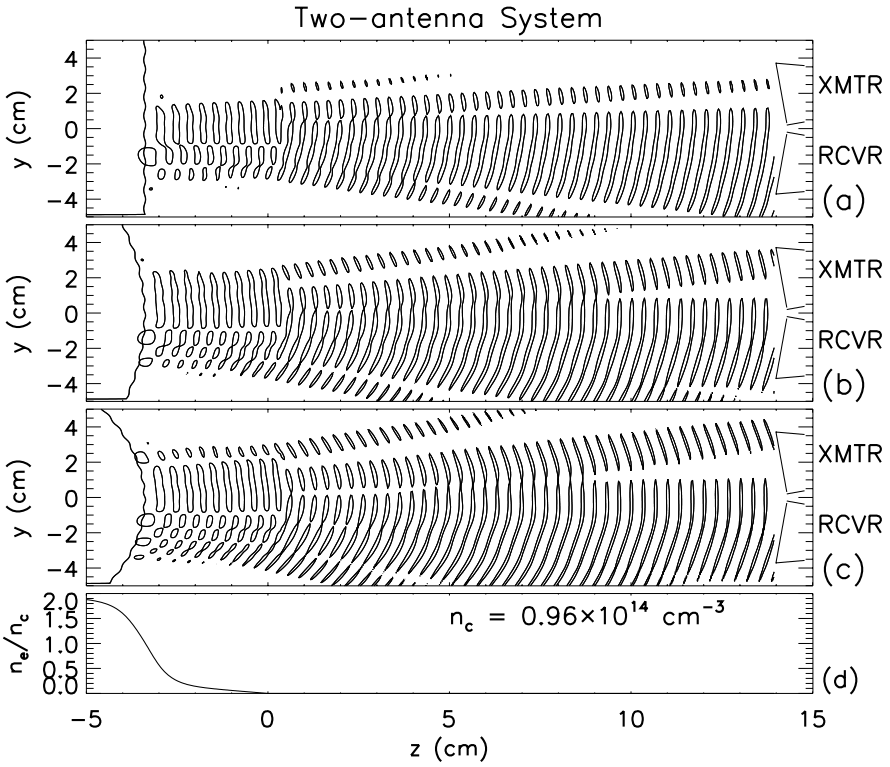

Figure 4: (Y. Lin)

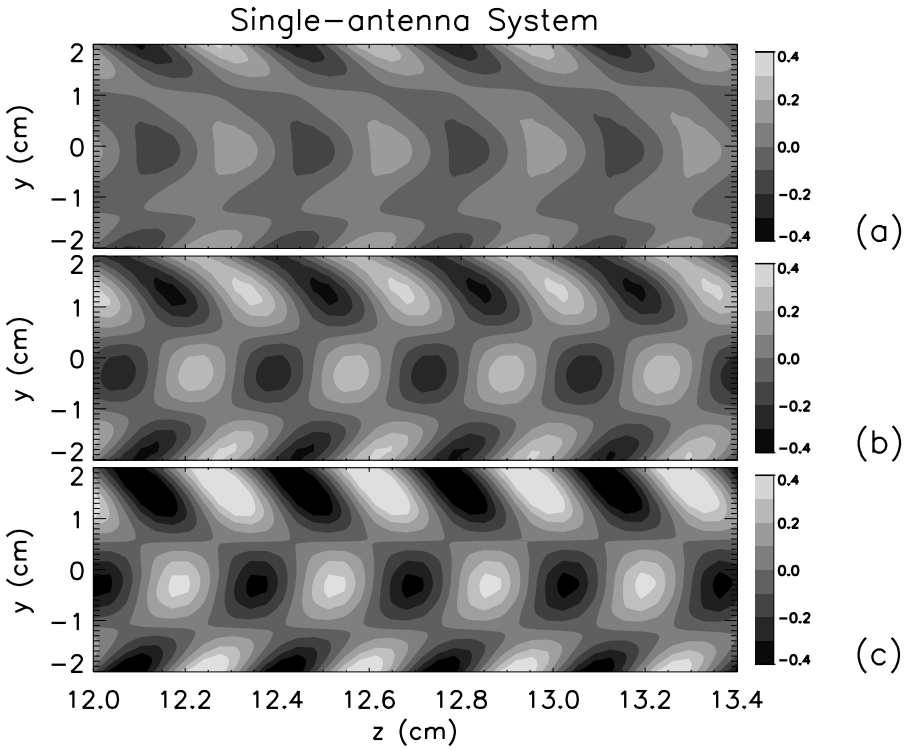

Figure 5: (Y. Lin)

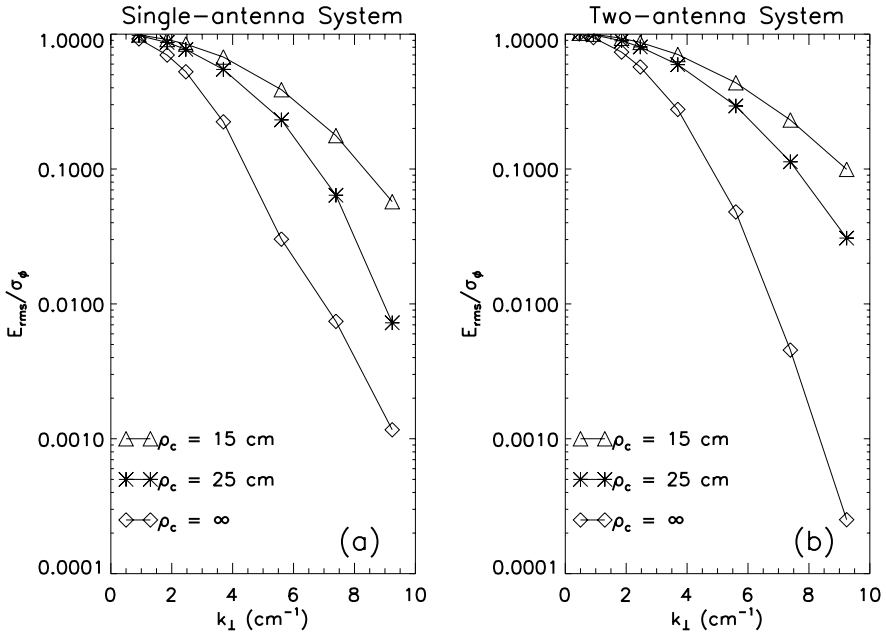

Figure 6: (Y. Lin)